

ZnO Nanoparticles-Reinforced Chitosan–Xanthan Gum Blend Novel Film with Enhanced Properties and Degradability for Application in Food Packaging

Zeba Tabassum, Madhuri Girdhar,* Anil Kumar, Tabarak Malik,* and Anand Mohan*



Cite This: *ACS Omega* 2023, 8, 31318–31332



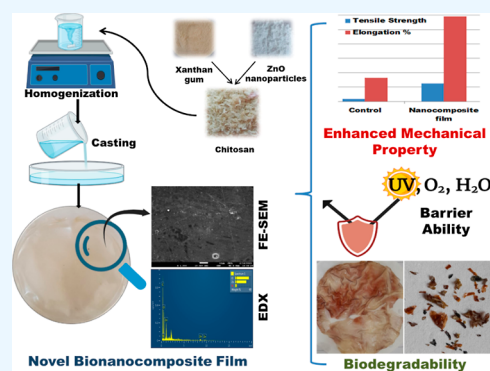
Read Online

ACCESS |

Metrics & More

Article Recommendations

ABSTRACT: Nations all over the world are imposing ban on single-use plastics, which are difficult to recycle and lead to creations of nonsustainable and nondegradable piles. To match the requirement in the market, suitable food packaging alternatives have to be developed that are biodegradable and environment-friendly. The current work is designed for the fabrication of a novel nanocomposite by blending xanthan gum in a chitosan matrix and reinforcing it with ZnO nanoparticles, through a solution casting method. Surface morphology of the film was investigated through field emission scanning electron microscopy, along with energy-dispersive X-ray spectroscopy mapping, and characterized through thermogravimetric analysis, Fourier transform infrared (FTIR) spectroscopy, mechanical testing, and ultraviolet spectroscopy. FTIR spectroscopy analysis corroborated the interaction between the components and the H-bond formation. Polyelectrolyte complex formation materializes between the oppositely charged chitosan and xanthan gum, and further nanoparticle incorporation significantly improves the mechanical properties. The synthesized nanocomposite was found to have increases in the tensile strength and elongation at break of pure chitosan by up to 6.65 and 3.57 times, respectively. The transmittance percentage of the bionanocomposite film was reduced compared to that of the pure chitosan film, which aids in lowering the oxidative damage brought on by UV radiation in packed food products. Moreover, the film also showed an enhanced barrier property against water vapor and oxygen gas. The film was totally biodegradable in soil burial at the end of the second month; it lost almost around 88% of its initial weight. The fabricated film does not pose a threat to the environment and hence has great potential for application in the future sustainable food packaging industry.



INTRODUCTION

Fresh agriculture products are perishable items, and the primary causes of their quality decline and shorter shelf life includes physical damage, moisture loss, and microbial attack after harvest.¹ The main objective of the food packaging is to protect food goods from ultraviolet (UV) light, oxygen, moisture, and microorganisms, as well as to increase their shelf life by shielding them from liquids, odors, and other contaminants during transportation, handling, and storage.² Fossil-based polymer packages have become an essential component of modern life due to their wide range of desired qualities and ease of manufacture. However, this straightforward manufacturing and applicability also leads to the generation of one of the most nonsustainable types of waste because it is nondegradable in nature, typically designed for single use, and is extremely difficult to sort and recycle.³ A major amount of plastic trash is improperly disposed of due to inadequate or nonexistent plastic waste management systems.⁴ One of the significant issues presented by the United Nations (UN) climate change conference (COP26) is the severe changes to the global climate due to the unacceptably

increasing rate of plastic usage. According to estimates, the carbon emissions from plastics alone makes around 15% of global carbon dioxide emissions, or roughly 1.7 gigatons of CO₂. If no stringent action is taken, this number is anticipated to quadruple by 2050.⁵ Several countries are imposing bans on the production, import, storage, distribution, sale, and use of single-use plastic for the increasing difficulty to dispose of this waste as well as due to their adverse impacts on the environment and public health caused by contaminating land and water resources and even entering the food chain. This has led to an increased need to solve this global concern by finding an environmentally acceptable alternative material for packaging that is affordable, convenient, and eco-friendly.^{4,6} Biobased polymers are physically and functionally comparable

Received: May 29, 2023

Accepted: August 3, 2023

Published: August 17, 2023

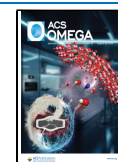


Table 1. Components and Composition Used to Prepare All the Films

s. no	chitosan (%)	xanthan gum	ZnO nanoparticles (wt %)	remarks	film code
1	1	NA	NA	good transparent film; selected	C
2	1	0.5%	NA	good transparent film; selected	CX
3	1	1.0%	NA	decreased transparency; rejected	NA
4	1	1.5%	NA	brittle film; rejected	NA
5	1	0.5%	1	good transparent film; selected	CXZ1
6	1	0.5%	3	good transparent film; selected	CXZ3
7	1	0.5%	5	good transparent film; selected	CXZ5
8	1	0.5%	7	decreased transparency and brittleness/stiffness; rejected	NA

to petroleum-based polymers; they are also less expensive, biodegradable, and abundantly available from renewable resources.³ However, as compared to traditional plastic packaging, biopolymers derived from plants, animals, and microorganisms have slightly inferior physiochemical and mechanical properties.⁷ The reinforcement of nanomaterials, plasticizers, other biopolymers, plant extracts/essential oils, etc. can address these limitations, while also improving other functional properties.^{8,9}

Chitosan is one such biopolymer with natural film-forming ability, nontoxic property, inherent antimicrobial activity, abundant availability, and biodegradability.^{10,11} It is a linear cationic heteropolysaccharide biopolymer ($C_{56}H_{103}N_9O_{39}$) containing deacetylated β -(1-4)-D-glucosamine and acetylated *N*-acetyl-D-glucosamine, derived from the deacetylation of chitin, a major byproduct of the shellfish industry, present in the exoskeletons of crabs, shrimps, and other crustaceans.^{12,13} Commercially manufactured chitosan typically has a molecular weight that ranges from 3800 to 20,000 Da on average. As a byproduct of the seafood business, it provides an inexpensive approach to being used as raw material in the food packaging sector by supporting industrial symbiosis.³ Along with its so many advantages, chitosan also possesses some inherent limitations that include lower mechanical strength and hydrophilicity.^{14,15} According to research, there is a good probability that the addition of nanofillers or other biopolymers can improve the material's qualities and applications. Chitosan blends and nanocomposites generally have enhanced mechanical characteristics, moisture restriction, and the ability to act as a gas barrier.^{5,16,17} Xanthan gum [$(C_{35}H_{49}O_{29})_n$] is another polysaccharide biopolymer (branched heteropolysaccharide) with a high molecular weight (2×10^6 to 10^7), composed of pentasaccharide units (2:2:1 molar ratio of D-glucose, D-mannose, and D-glucuronic acid residues), and has been a very popular compound in recent years for its common usage as a food additive, a stabilizer, and a thickener.¹⁸ According to various published reports, xanthan gum addition has the ability to improve various characteristics of other biopolymers including the mechanical ability¹⁹ and antioxidant and antibacterial activities.²⁰ Several studies have revealed that the pure polysaccharides and their composite polymer films containing metal oxide nanoparticles such as ZnO nanoparticles possess moderate to very good antibacterial activity²¹ and have been proven to impart good thermal stability, enhanced hydrophobicity,^{22,23} and decreased solubility,²⁴ even in some cases a better barrier ability than the commercial packages have obtained.²⁵⁻²⁷

The present study was aimed to fabricate chitosan/xanthan gum blend films incorporated with ZnO nanoparticles through the solution casting method and investigate their nanostructure and functional properties for their potential use in biodegrad-

able food packaging applications, which has not been studied or reported before. Although chitosan, xanthan gum, and ZnO nanoparticles have been separately used by researchers, the authors expect chitosan/xanthan gum/ZnO nanoparticles as a new combination to achieve a significant enhancement in packaging material properties, i.e., strength, flexibility, water resistance, barrier ability, etc., to compete with plastic packaging. Chitosan and xanthan gum being oppositely charged are expected to interact efficiently, and polyelectrolyte formations are likely to happen, which can lead to an increased mechanical ability of chitosan in terms of strength and flexibility. Further, reinforcement with ZnO nanoparticles can lead to mechanical, thermal barrier, and antimicrobial efficacy. So, it is predicted to develop into a novel combination of high-performance biobased packaging material with high degradability.

EXPERIMENTAL SECTION

Materials. Chitosan from shrimp shells, 75% deacetylated, was bought from Loba Chemie Pvt. Ltd., India. Xanthan gum pure (Food grade), glacial acetic acid (99.5% extra pure), and glycerol (purified) were also procured from Loba Chemie Pvt. Ltd., India. Zinc oxide nanopowder was purchased from Sigma-Aldrich (<100 nm particle size). Anhydrous $CaCl_2$ and NaCl were obtained from Loba Chemie Pvt. Ltd., India. High-glucose Dulbecco's modified Eagle medium (DMEM), fetal bovine serum, MTT reagent, and Dulbecco's phosphate buffered saline (D-PBS) were purchased from Himedia, and dimethyl sulfoxide (DMSO) was procured from Sigma.

Preparation of Films. All the films were fabricated through a solution casting method as it is the most extensively utilized method for fabrication of chitosan-based nanocomposite films due to its low cost and ease of preparation. Research suggests that a longer drying time in lower temperature results in reorganization of the solution structure and effective interactions due to hydrogen bonds and van der Waals forces between the water molecules and hydrophilic tails of the chitosan.²⁸ Table 1 represents all of the components and their composition. A total of five types of films were successfully prepared through the solution casting method, which are the pure chitosan film (C) as the control, chitosan/xanthan gum blend (CX), and chitosan/xanthan gum blend incorporated with ZnO nanoparticles 1 wt % (CXZ1), 3 wt % (CXZ3), and 5 wt % (CXZ5). The chitosan film was prepared following the methodology described by Cazón and Vázquez.²⁹ To prepare the 1% pure chitosan film, 1 g of chitosan flakes was dissolved in 100 mL of aqueous solution containing 1% glacial acetic acid and kept on a magnetic stirrer at room temperature for an hour to completely dissolve and form a transparent solution. Further, the solution was poured in a Petri dish and left to dry.

Xanthan gum solutions were prepared by the slow addition of the xanthan gum powder in distilled water under continuous stirring by a magnetic stirrer at room temperature for half an hour.³⁰ Chitosan/xanthan gum blend was prepared following the method described by de Moraes Lima et al.¹⁹ The dissolution of xanthan gum and chitosan was mixed with the addition of glycerol as a plasticizer at a concentration of 0.30 g glycerol/g polymer. The dispersion was further subjected to homogenization for 10 min. The resultant homogenized solution was cast on a Petri dish and left to dry at room temperature.

Chitosan/xanthan gum/ZnO bionanocomposite films were prepared following the methodology described by other researchers, with a slight modification.^{31,32} First of all, chitosan/xanthan gum blend solution was prepared through homogenization, and then, ZnO nanoparticle loading was conducted in the resultant solution, which was kept on a magnetic stirrer overnight, followed by at least 10 min degasification in an ultrasound bath. The mixed solution was further poured in Petri dishes and dried for at least 48 h. All the films were carefully peeled off after drying and kept in a desiccator until the start of other experiments.^{19,32}

Characterization. Thickness and Transparency. Thickness measurement of all of the thin films was performed. SEM images were taken at different places using field emission scanning electron microscopy (FE-SEM) (JEOL), and the average thickness was calculated.

The transparency of the film was calculated by using the formula $T = \text{Abs}_{600}/X$, where T is the transparency, Abs_{600} is the film's absorbance at 600 nm, and X is the thickness of the film in millimeters.^{22,27}

Field Emission Scanning Electron Microscopy, Energy-Dispersive X-ray Spectroscopy, and Mapping. To assess the surface morphology of the films, FE-SEM (JEOL) was performed, and images were obtained at different magnifications and accelerated voltages of 5 and 10 kV. SEM is performed in combination with EDS/EDX (energy-dispersive X-ray spectroscopy) and mapping to identify and characterize the elemental composition. All the films were coated with a conductive layer of gold in order to prevent charging of the surface.

Fourier Transform Infrared Spectroscopy. Fourier transform infrared (FTIR) spectroscopy was employed to understand the preliminary structures of the fabricated films and the interaction of the components. FTIR spectroscopy was performed in the transmission mode by using an FTIR spectrometer (PerkinElmer: Spectrum 10 software, 0.5 cm^{-1} resolution) in the range of 400–4000 cm^{-1} .

Mechanical Capability Analysis. Mechanical properties (tensile strength and elongation-at-break) of the films were assessed using a universal testing machine (Zwick Roell, Germany Static UTM Z010), according to the standards of ASTM, at room temperature with a cross head speed of 10 mm/min.

Thermogravimetric Analysis. Thermal stability of all the films was investigated through thermogravimetric analysis (TGA), and its respective derivative thermogravimetric (DTG) curve was drawn. TGA was carried out utilizing a thermogravimetric analyzer (PerkinElmer) in the temperature range from 30.00 °C to 500.00 °C at a heating rate of 10 °C/min in a nitrogen atmosphere (20 mL/min).

Water Vapor Transmission Rate. The films' water vapor transmission rate (WVTR) was measured using the ASTM E96

method.²² The sample films were mounted tightly on the mouth of a glass vial (1 cm diameter) containing preweighed anhydrous calcium chloride (CaCl_2), and the vials were placed in a desiccator maintaining $75 \pm 5\%$ relative humidity with a saturated sodium chloride (NaCl) solution at 30 ± 2 °C. The vials were weighed before and after 1 day, and the film's WVTR was calculated using the formula mentioned below

$$\text{WVTR}(\text{g}/\text{m}^2/\text{day}) = W/S$$

where W is the weight gain of the glass vial after 1 day and S is the exposed surface area of the film.

Water Absorption Capacity. The water absorption capacity of all the films was examined by cutting the film to the size of 2 cm \times 2 cm, weighing (initial weight = W_1), and then immersing entirely in deionized water for 24 h for water absorption. After sufficient swelling, the films were taken from the water, any excess water on the film surface was wiped using filter paper, and the final weight (W_2) was measured. The water absorption capacity of the films were determined by using the formula mentioned below^{24,33}

$$\text{water absorption capacity}(\%) = \frac{W_2 - W_1}{W_1} \times 100$$

Oxygen Transmission Rate and Permeability. Gas barrier properties of the films were checked through an oxygen transmission test. The oxygen permeability analysis was carried out using the method described by other researchers.^{24,33} The 2 cm \times 2 cm films were wrapped around the mouth of the glass vial and sealed with a strip. Following that, the bottles were placed in a desiccator at room temperature. Over a 3 day period, the mass of each bottle was measured once a day. The following equations were used to calculate the OPTR (oxygen permeability transmission rate) and OP (oxygen permeability)

$$\text{OPTR} = \text{slope}/\text{film area}$$

$$\text{OP} = \text{OPTR} \times L/\Delta P$$

where ΔP is the partial vapor pressure difference between pure water and the dry atmosphere (0.02308 atm at 25 °C) and L represents the average film thickness.

UV Barrier. The absorbance of the films was measured using a UV–visible spectrophotometer (280–800 nm) to determine the UV light barrier property. The test films were cut into rectangular pieces (3 cm \times 1 cm) and positioned in a quartz cuvette for spectrophotometric analysis. An empty cuvette was used as control.²⁴

Biodegradation. Biodegradation test was carried out indoor by burying the films with soil and calculating weight loss as per the method reported by other researchers in the case of degradability check of biopolymer-based films.^{22,24} To maintain the moisture/humidity in soil, tap water was sprinkled once a day, and the excess water was flushed through a drainage in the pot's bottom. All of the films were preweighed (W_i) before being buried in fresh soil collected from a field in a 10 L pot. The biodegradation of the film samples was measured at 7 day intervals by gently removing the sample from the soil and rinsing it with distilled water to remove the soil from the film, followed by drying by keeping it in a desiccator and weighing (W_f). Degradation or weight loss % of the film was further calculated using the following formula.

Table 2. Different Properties/Characteristics of all the Films^a

s. no	film	thickness	opacity	tensile strength (MPa)	elongation at break (%)	water vapor transmission rate (WVTR) in g/m ² /day	water absorption capacity (%)	oxygen transmission rate (OTR) (cm ³ /m ² /day)	oxygen permeability (OP) (cc/m ² ·24 h·atm)
1	C	0.05 ± 0.003 ^c	3.16 ± 0.15 ^b	3.67 ± 1.00 ^c	33.17 ± 1.75 ^d	560.93 ± 1.94 ^a	75.68 ± 1.84 ^a	1910.64 ± 1.15 ^a	4.12 ± 0.01 ^e
2	CX	0.06 ± 0.010 ^c	3.33 ± 0.15 ^b	5.68 ± 1.43 ^c	14.73 ± 1.39 ^e	494.26 ± 2.54 ^b	68.60 ± 0.38 ^b	1846.92 ± 0.57 ^b	4.78 ± 0.02 ^d
3	CXZ1	0.08 ± 0.003 ^b	3.43 ± 0.4 ^b	20.94 ± 1.65 ^{ab}	63.60 ± 1.25 ^b	270.48 ± 2.65 ^d	31.07 ± 1.56 ^d	1630.57 ± 0.44 ^d	5.62 ± 0.025 ^c
4	CXZ3	0.09 ± 0.005 ^{ab}	4.7 ± 0.3 ^a	24.42 ± 1.26 ^a	118.6 ± 1.52 ^a	252.65 ± 2.64 ^e	30.36 ± 1.2 ^e	1579.6 ± 0.28 ^e	6.15 ± 0.025 ^b
5	CXZ5	0.10 ± 0.011 ^a	5.17 ± 0.2 ^a	20.13 ± 2.25 ^b	53.34 ± 2.56 ^c	296.29 ± 2.76 ^e	55.11 ± 1.75 ^c	1809.03 ± 0.96 ^e	7.86 ± 0.03 ^a

^aMeans that do not share a letter are significantly different values at ($p \leq 0.05$) using the Tukey test (mean ± SD, $n = 3$).

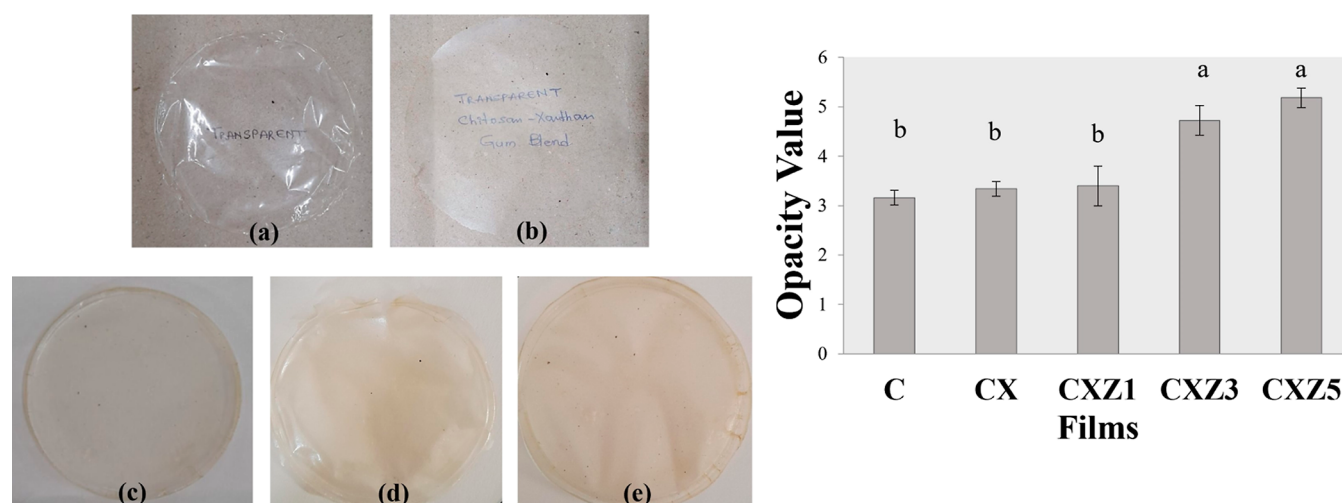


Figure 1. All synthesized films and their opacity values [means that do not share a letter are significantly different values at ($p \leq 0.05$) using the Tukey test (mean ± SD, $n = 3$)] (a) C is the pure chitosan film, (b) CX is the chitosan/xanthan gum blend film, (c) CXZ1 is the chitosan/xanthan gum blend incorporated with 1 wt % ZnO nanoparticles, (d) CXZ3 is the chitosan/xanthan gum blend incorporated with 3 wt % ZnO nanoparticles, and (e) CXZ5 is the chitosan/xanthan gum blend incorporated with 5 wt % ZnO nanoparticles. [All the digital photos of the films are original, taken and presented by the author Zeba Tabassum.]

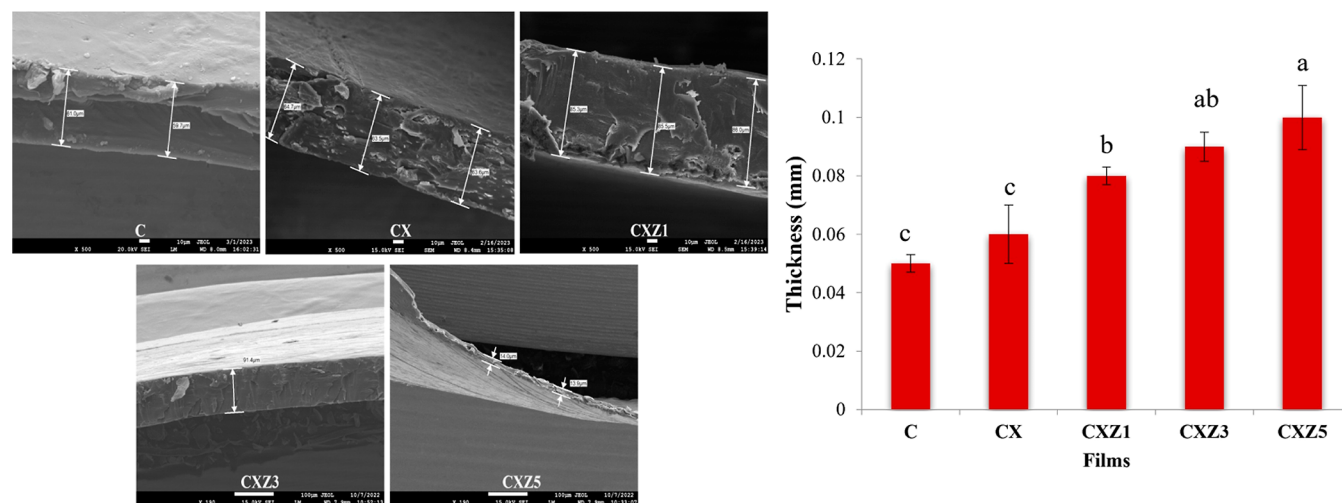


Figure 2. Thickness of all the manufactured films [means that do not share a letter are significantly different values at ($p \leq 0.05$) using the Tukey test (mean ± SD, $n = 3$)] (C is the pure chitosan film, CX is the chitosan/xanthan gum blend film, CXZ1 is the chitosan/xanthan gum blend incorporated with 1 wt % ZnO nanoparticles, CXZ3 is the chitosan/xanthan gum blend incorporated with 3 wt % ZnO nanoparticles, and CXZ5 is the chitosan/xanthan gum blend incorporated with 5 wt % ZnO nanoparticles).

$$\text{Degradation \% or Weight Loss \%} = \frac{W_i - W_f}{W_i} \times 100$$

where W_i and W_f are the initial weight of the film sample and the final weight of the film sample, respectively.

Cytotoxicity of the CXZ3 Film. CXZ3 seemed to be the best ratio film considering all of the previous characterization results. According to the ISO 10993:5 standard procedure, the MTT assay was used to test the cytotoxicity of the CXZ3 film against L929 cells. PBS solution was used to assess the film

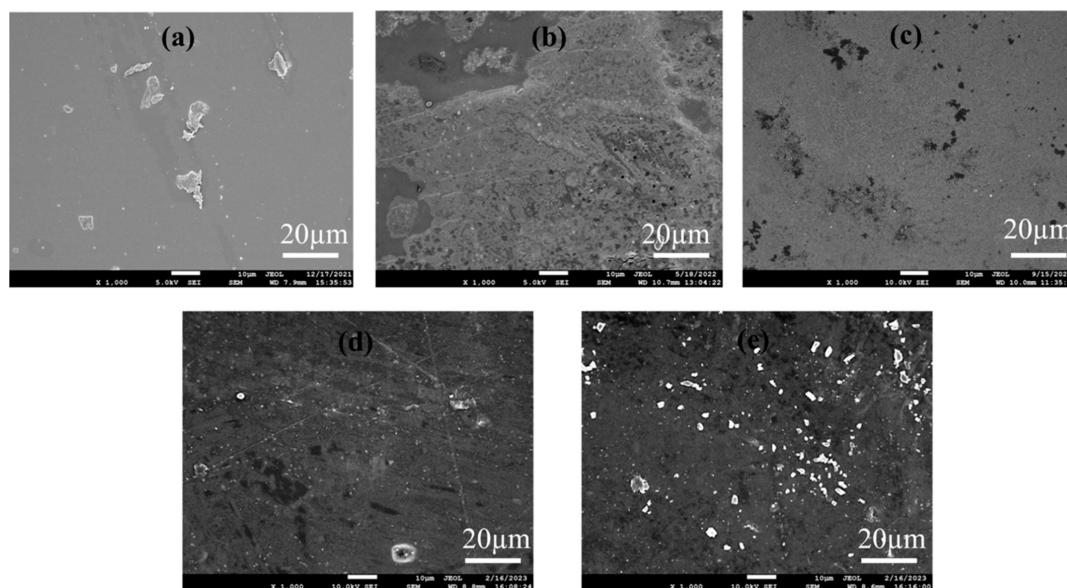


Figure 3. SEM images of all the films: (a) C is the pure chitosan film, (b) CX is the chitosan/xanthan gum blend film, (c) CXZ1 is the chitosan/xanthan gum blend incorporated with 1 wt % ZnO nanoparticles, (d) CXZ3 is the chitosan/xanthan gum blend incorporated with 3 wt % ZnO nanoparticles, and (e) CXZ5 is the chitosan/xanthan gum blend incorporated with 5 wt % ZnO nanoparticles.

extracts. The optical density (OD) was measured using a spectrophotometer at a wavelength of 570 nm. Cell viability and cytotoxicity were calculated as described by Saral and co-workers.²⁵

Statistical Analysis. The data were obtained in triplicate for each experiment and were analyzed statistically. One-way analysis of variance (ANOVA) and the Tukey test ($p \leq 0.05$) were used to identify differences between the mean values in the data, which were expressed as the mean standard deviation, utilizing OriginPro 2021.

RESULTS AND DISCUSSION

Among the blended biopolymer films, 1% chitosan + 0.5% xanthan gum proved to be a suitable film through visual examination. The rest of the films (1 and 1.5% of xanthan added to 1% chitosan separately) with an increasing amount of xanthan gum were rejected due to less smoothness and less transparency. The chosen blend films were further reinforced with 1, 3, 5, and 7% ZnO nanoparticles. However, the 7% nanocomposite film was rejected due to its decreased transparency and brittleness, and the remaining films were subjected to further experimentation (Table 1).

All the films appeared glossier on the lower side than on the upper side because of the evaporation of water from the upper surface of the film in the casting tray. Zhou and co-workers observed similar characteristics in their fabricated film.³⁴

Thickness and Transparency. A key factor in influencing the film's physical characteristics (such as optical and barrier property) is its thickness. Pure biopolymer, biopolymer blend, or a different ratio of nanocomposite films did not alter the thickness significantly; however, it increased slightly from 0.05 mm (C) to 0.1 mm (CXZ5). The measured thicknesses are listed in Table 2. An increase in the components and ratio exhibited a positive correlation with the thickness, as depicted in Figure 2 (bar graph). Figure 2 also represents some of the SEM micrographs measuring the thickness of the films.

Digital images of all the fabricated films are shown in Figure 1. Food packaging film's transparency is crucial for both

customer appeal and visual monitoring of the product during storage. Transparency values are shown in Figure 1 and are tabulated in Table 2. The C film was found to be the least opaque (the most transparent). Addition of xanthan gum and ZnO nanoparticles decreased the transparency to some extent. As the amount of ZnO nanoparticles in the nanocomposite films increased, so did their opacity. The CXZ1, CXZ3, and CXZ5 films were found to have opacity values of 3.4, 4.7, and 5.1, respectively, which suggests that the ZnO nanoparticles scattered in them was to blame for the reduction in transparency (the lower the opacity value, the higher the transparency). A similar observation has been reported by other scientists.^{22,25} However, all of the films were revealed to be transparent and not entirely opaque through visual inspection.

FE-SEM, EDX, and Mapping. To evaluate the surface morphology of the created films, SEM analysis was conducted, and the resultant micrographs are depicted in Figure 3. The SEM image of pure chitosan revealed a smooth and homogeneous surface with small clusters, which are agglomerates of chitosan molecules/undissolved small chitosan particles. Several publications noted comparable outcomes.^{9,24,35} The surface of bionanocomposites (CXZ1, CXZ3, and CXZ5) clearly appeared to have dispersed nanofillers. Surface roughness of the nanocomposite films with the presence of nanoparticles steadily increases as the nanofillers ratio increases (CXZ1 < CXZ3 < CXZ5). The CXZ3 film surface seems to have the most homogeneous distribution of nanoparticles (Figure 3d), which is suitable to achieve compatibility between the filler and matrix, which eventually can lead to an enhancement of film characteristics. This is in agreement with other properties improvements of the film. The nanoparticles started to aggregate as the ZnO level was increased to 5 wt % (Figure 3e). This is in agreement with the observation of other scientists, where after a certain ratio, nanofillers start to form agglomeration.²⁵

The EDX spectrum of the nanocomposite (CXZ3) film in Figure 4a unveils the presence of elements Zn and O, which is

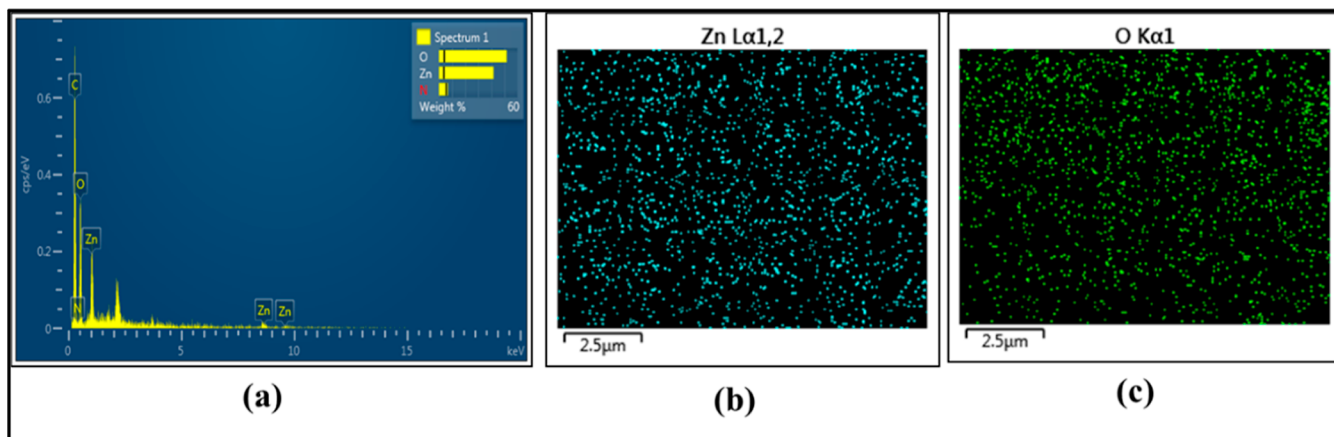


Figure 4. EDX and mapping of the CXZ3 nanocomposite (chitosan/xanthan gum blend incorporated with 3 wt % ZnO nanoparticles): (a) EDX mapping showing the presence of elements Zn and O and (b,c) showing the distribution of Zn and O.

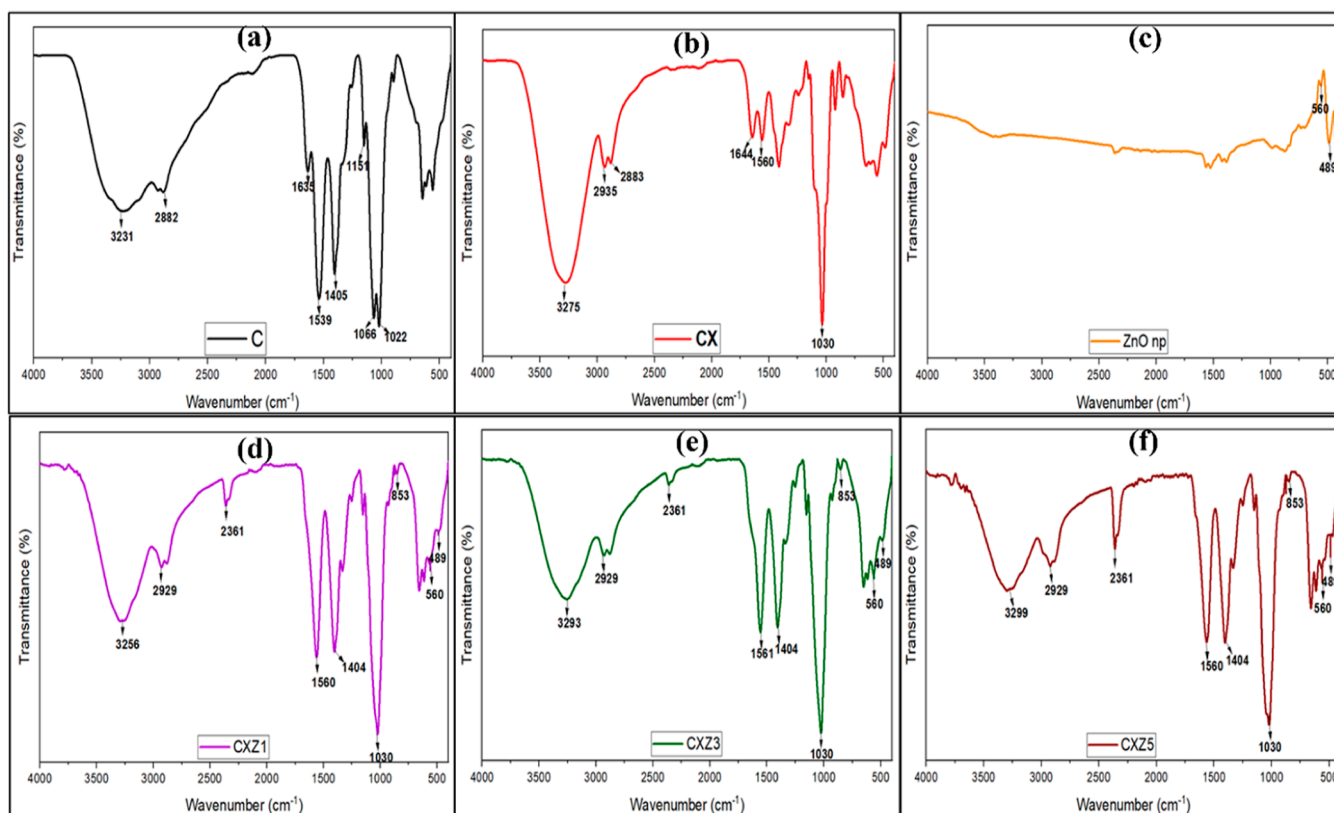


Figure 5. FTIR spectroscopy analysis of all the films [(a) C is the pure chitosan film, (b) CX is the chitosan/xanthan gum blend film, (c) ZnO nanoparticles, (d) CXZ1 is the chitosan/xanthan gum blend incorporated with 1 wt % ZnO nanoparticles, (e) CXZ3 is the chitosan/xanthan gum blend incorporated with 3 wt % ZnO nanoparticles, and (f) CXZ5 is the chitosan/xanthan gum blend incorporated with 5 wt % ZnO nanoparticles].

attributed to the ZnO nanoparticles that are present in the nanocomposite films. Mapping (Figure 4b,c) confirmed the relatively homogeneous distribution of the elements Zn and O.

Fourier Transform Infrared Spectroscopy. To determine the structural properties of the films, FTIR spectroscopy was performed. Based on Figure 5, we can observe that film C (Figure 4 a) has the band at 3231 cm^{-1} , which refers to the stretching vibration of free hydroxyl ($-\text{OH}$), as well as to symmetric and asymmetric stretching of $\text{N}-\text{H}$ bonds in the amino group present in the chitosan molecules.^{25,36} 2882 cm^{-1} suggests the presence of the $\text{C}-\text{H}$ bond. The bands at 1635

and 1539 cm^{-1} were due to $\text{C}=\text{O}$ stretching (amide I band) and $\text{N}-\text{H}$ bending (amide II band), respectively.^{22,37} The peaks at 1405 cm^{-1} indicate vibrational modes of symmetric deformation of the CH_2 group.³⁸ 1151 cm^{-1} is related to asymmetric vibrations of CO in the oxygen bridge resulting from deacetylation of chitosan.³⁹ The peaks at 1066 cm^{-1} and at 1022 cm^{-1} are associated with the vibrational modes by stretching of the groups $-\text{OH}$, $3'-\text{OH}$, and $5'-\text{OH}$ ⁴⁰ in chitosan molecules. Also, the $\text{C}-\text{O}$ bond is related to the 1022 cm^{-1} peak.⁹ All these functional groups mentioned above are expected to be present in the chitosan spectrum.¹⁹

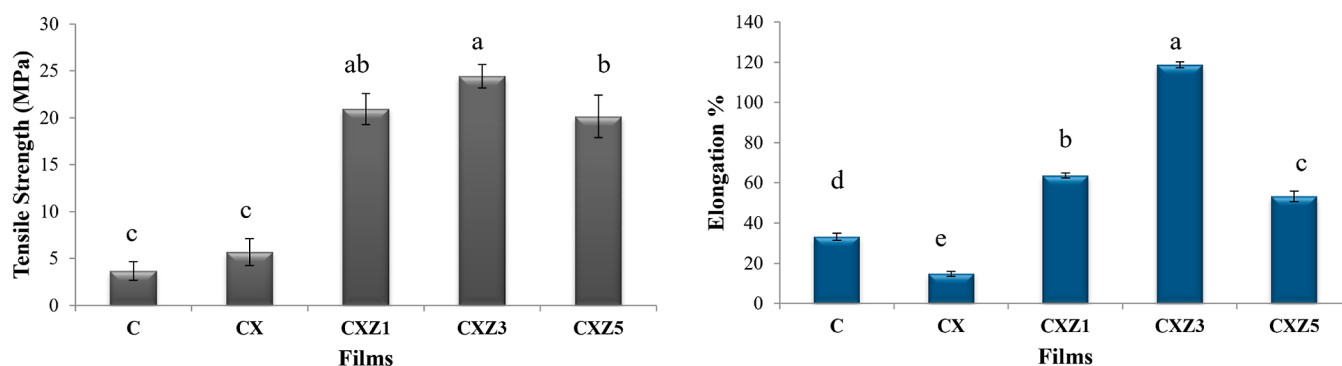


Figure 6. Mechanical property (tensile strength and elongation at break) of all the films [means that do not share a letter are significantly different values at ($p \leq 0.05$) using the Tukey test (mean \pm SD, $n = 3$)] [C is the pure chitosan film, CX is the chitosan/xanthan gum blend film, CXZ1 is the chitosan/xanthan gum blend incorporated with 1 wt % ZnO nanoparticles, CXZ3 is the chitosan/xanthan gum blend incorporated with 3 wt % ZnO nanoparticles, and CXZ5 is the chitosan/xanthan gum blend incorporated with 5 wt % ZnO nanoparticles].

In the case of the chitosan/xanthan gum blend film (CX), the peak at 3275 cm^{-1} indicates O–H stretching and H bonding. This peak was shifted a little higher than that in pure chitosan, suggesting intermolecular hydrogen bonding between the components of the blended films. This is in resemblance with the report stated by Saral et al. in their paper.²² 2883 and 2935 cm^{-1} suggest a strong N–H stretch. The peak at 1560 cm^{-1} indicates the presence of COO^- of xanthan gum, and 1644 cm^{-1} suggests N–H bending of chitosan. These confirm the chance of formation of a complex system by oppositely charged two polyelectrolyte biopolymers, which resulted in a proper biopolymer blend matrix. A similar peak was observed in the chitosan/xanthan gum blend of de Morais Lima and colleague's work.¹⁹ Peaks at 1066 and 1022 cm^{-1} were absent in blend nanocomposites, indicating bond formation with the functional group (OH) (Figure 5b).

In all the ZnO nanocomposite films (Figure 5d–f), the addition of ZnO nanoparticles in the biopolymer blend matrix shows that the peak corresponding to the –OH group is shifted to a higher wavenumber (3256 , 3293 , and 3299 cm^{-1}), which is expected from ZnO nanoparticles, and this phenomenon may be related to the generation of strong hydrogen bonds between fillers and the biopolymer matrix.⁹ All the nanocomposite films showed similar peaks; however, the intensity is lower in CXZ5, which could be attributed to the agglomeration of nanofillers that typically reduce its interaction with the biopolymer matrix.⁴¹ The peak at 2929 cm^{-1} indicates the O–H stretch and intermolecular bonding. 2361 cm^{-1} corresponds to possibilities of C–H stretch, C=O stretch, and –OH stretches. The band at 1404 cm^{-1} represents O–H bending and the 1560 cm^{-1} peak is for the presence of xanthan gum.¹⁹ Peak at 853 cm^{-1} is corresponding to the presence of ZnO nanoparticles in the composite film. 489 cm^{-1} represents the stretching mode of ZnO and confirms the presence of ZnO nanoparticles in the composite.⁴² FTIR spectroscopy analysis of ZnO nanoparticles showed similar peaks, as shown in Figure 5c.

So, all the nanocomposites confirm the presence of chitosan and xanthan gum as well as the filler in the film. FTIR spectroscopy analysis also indicates that strong intermolecular bonding occurred between the components, which suggests fine compatibility. There is a high chance of polyelectrolyte complex formation by chitosan and xanthan gum, with oppositely charge functional groups.

Mechanical Studies. Mechanical properties are critical parameters to determine the precise function of a polymer film in terms of its strength and flexibility as it must be able to endure the regular stress encountered during its practical application and must be able to protect the food item during distribution, transport, or storage. A higher elongation usually indicates a higher-grade material when combined with a good tensile strength. Table 2 summarizes the strength and elongation at break of pure chitosan (C), chitosan/xanthan gum blend (CX), and the bionanocomposite films of various weight percentages (CXZ1, CXZ3, and CXZ5). In Figure 6, we can observe that the pristine chitosan (C) film possesses the lowest tensile strength, along with good elongation. Researchers blame chitosan's inherent hydrophilicity nature for its low mechanical capabilities.²² An increase (from 3.67 to 5.68 MPa) in its strength was observed when xanthan gum is blended with the chitosan. These findings imply that the addition of xanthan gum to the chitosan films increased intermolecular interactions, increasing the cohesive force of the films. This strength enhancement is due to their oppositely charged functional group interaction and the possibility of formation of a polyelectrolyte complex that led to a decrease in its flexibility to some extent.¹⁹ Other scientists also found that increasing tensile strength is often due to the increased interaction between the components, resulting in enhanced strength and reduced flexibility.^{41,43} Further, the mechanical property of the films was significantly improved by the incorporation of ZnO nanoparticles into the chitosan/xanthan gum blend, demonstrating enhanced interaction between both the biopolymers and the nanofillers. The outcomes are consistent with earlier studies.^{44–46} The composite films that are made using nanoclays/fibers and other nanofiller reinforcements have reported better mechanical ability.^{47–50} The findings in this study demonstrate that all of the nanocomposites had higher tensile strengths than the pristine chitosan film (C). A greater surface area in the nanofiller encouraged interactions between nanoparticles and the polymer matrix, which improved the development of cross-linking between polymer chains, resulting in the emergence of stronger films.⁴¹ A gradual increase in the tensile strength was observed with the increasing ZnO nanoparticle incorporation ratio, with values of 20.94 and 24.42 MPa for CXZ1 and CXZ3, respectively. These results are better in terms of the tensile value than low-density polyethylene (8 – 10 MPa), ethylene vinyl alcohol (6 – 19 MPa), and polycaprolactone (4 MPa) and close to high-

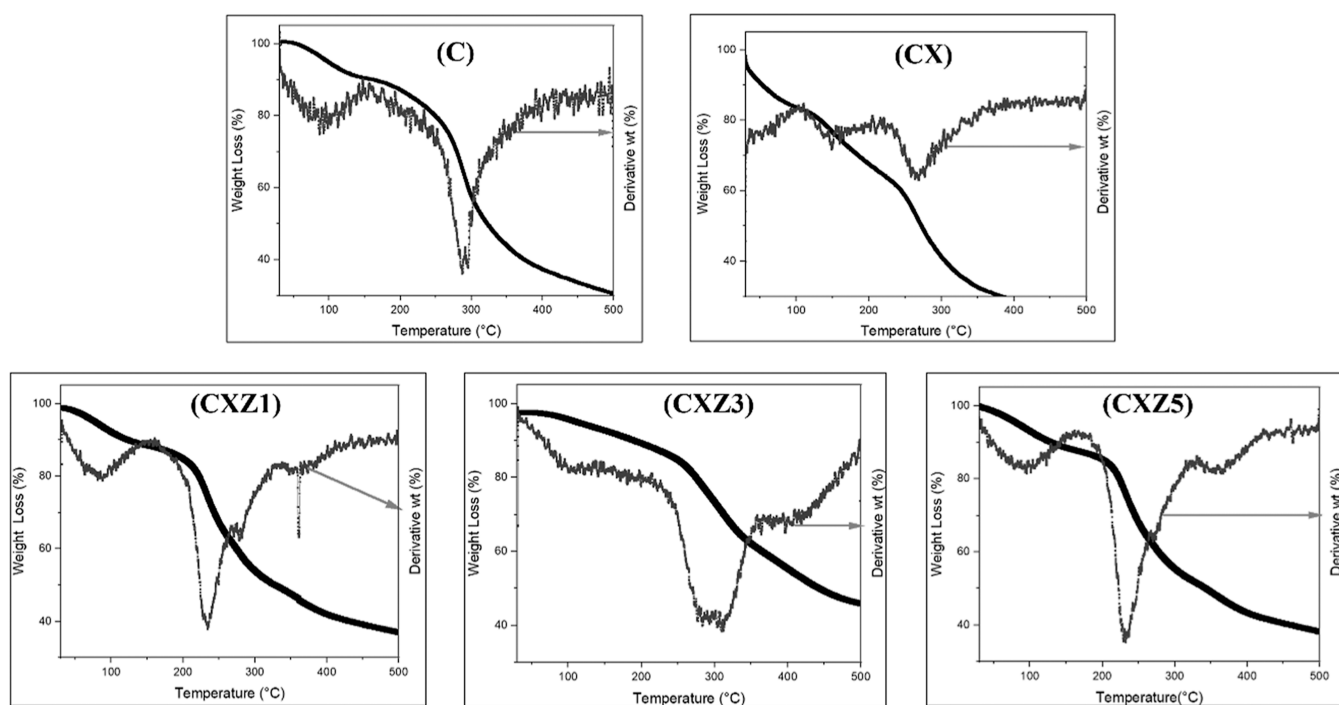


Figure 7. TGA–DTG thermographs of all the manufactured films (C is the pure chitosan film, CX is the chitosan/xanthan gum blend film, CXZ1 is the chitosan/xanthan gum blend incorporated with 1 wt % ZnO nanoparticles, CXZ3 is the chitosan/xanthan gum blend incorporated with 3 wt % ZnO nanoparticles, and CXZ5 is the chitosan/xanthan gum blend incorporated with 5 wt % ZnO nanoparticles).

density polyethylene (19–31 MPa).^{26,51} However, the tensile strength of the film started reducing with the additional loading of 5 wt % ZnO. This might have happened as a result of the excess ZnO adhering to the polymer blend matrix at this loading. This is in correspondence with the claim of Lomate and colleagues, in the case of the LDPE/Cu nanocomposite film.⁵² 3% (w/w) ZnO reached the highest (118.66%) elongation at break, much higher than that of the control. This implies that ZnO nanoparticles and tensile strength improvement show no interference with polymer chain mobility, even improving the stretchable mechanism, as suggested by other researchers.^{44,53} However, in both cases, tensile strength and elongation % first increase then start decreasing after a point; agglomeration of nanofillers is to be blamed.^{27,54} So, a ZnO loading of 3% might be regarded as ideal for producing the desired improvements in the mechanical characteristics. According to the findings of the FTIR investigation, the maximum amount of intermolecular hydrogen bonding between the nano ZnO filler and the chitosan/xanthan gum blend matrix may have taken place at this loading of ZnO. SEM micrographs disclose an improvement in homogeneity, along with an FTIR spectroscopy analysis report that reveals interactions with the functional groups. Less interface defects are obtained in the nanocomposite film as a result of the homogeneous dispersion of zinc oxide nanoparticles in the chitosan matrix, which inhibits molecular coagulation and enhances the tensile strength.⁵⁵ Many cyclic chain topologies on chitosan molecules make them particularly favorable to the creation of hydrogen bonds with –OH and –NH₂ groups. According to scientists, the mechanical characteristics enhancement of the chitosan-based films is due to these linkages, which can also make rotation and other chain molecular movements challenging. Furthermore, Rodrigues and co-workers concluded that ZnO nanoparticles

function as the chitosan molecule's interface coupling agents and offer higher energy intermolecular interaction, which even encourages the rotational movements of the molecular chains and increases the tensile strength of the film.⁹

Thermogravimetric Analysis. The thermal behavior of the synthesized packaging films was investigated as temperature can affect film stability. TGA determines how much a substance's mass changes when subjected to a controlled temperature program. Hence, TGA enables ascertaining information such as measuring the temperature range at which the sample acquires a fixed chemical composition as well as the rate at which dehydration, oxidation, combustion, and other reactions occur. The TGA/DTG curves for each sample scanned in a nitrogen environment are presented in Figure 7. According to the figure, in the thermogram of the C film, the initial thermal stage describes the release of water molecules attached to the functional groups (amino and hydroxyl groups) of the chitosan. The release, which constitutes 9.957% of the total chitosan mass, begins at 31.01 °C and continues till 170 °C. The second thermal stage represents the organic material loss and thermal degradation of chitosan molecules. This stage starts from 170 and continues till 425 °C, corresponding to a 54.075% mass loss. At the end, at 498.99 °C, chitosan was left with 30.406 wt %. All the other fabricated films have shown a similar kind of thermal stability when compared to the pure chitosan film, which exhibited similar types of decomposition curves. Among them, the CX film possessed a higher degradation rate, and the CXZ3 film was proven to have a slight improvement in terms of thermal stability. At the end, at 499.28 °C it was left with 45.74 weight %. Better interaction between the matrix and fillers is probably responsible for this marginal improvement.²⁷ Soni and co-workers also found not much difference in the TGA–DTG graph of all their fabricated films.⁵⁶

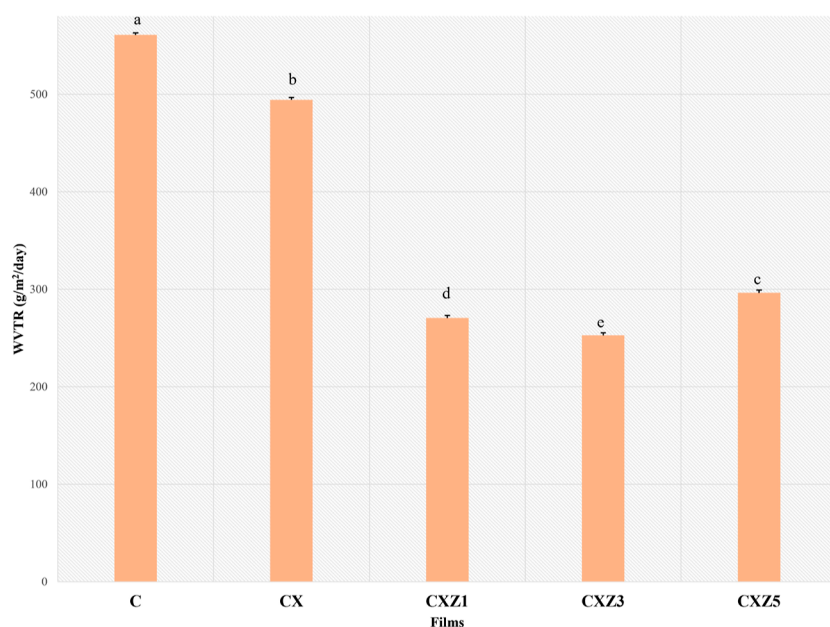


Figure 8. Rate of water vapor transmission of all the films [means that do not share a letter are significantly different values at ($p \leq 0.05$) using the Tukey test (mean \pm SD, $n = 3$)] (C is the pure chitosan film, CX is the chitosan/xanthan gum blend film, CXZ1 is the chitosan/xanthan gum blend incorporated with 1 wt % ZnO nanoparticles, CXZ3 is the chitosan/xanthan gum blend incorporated with 3 wt % ZnO nanoparticles, and CXZ5 is the chitosan/xanthan gum blend incorporated with 5 wt % ZnO nanoparticles).

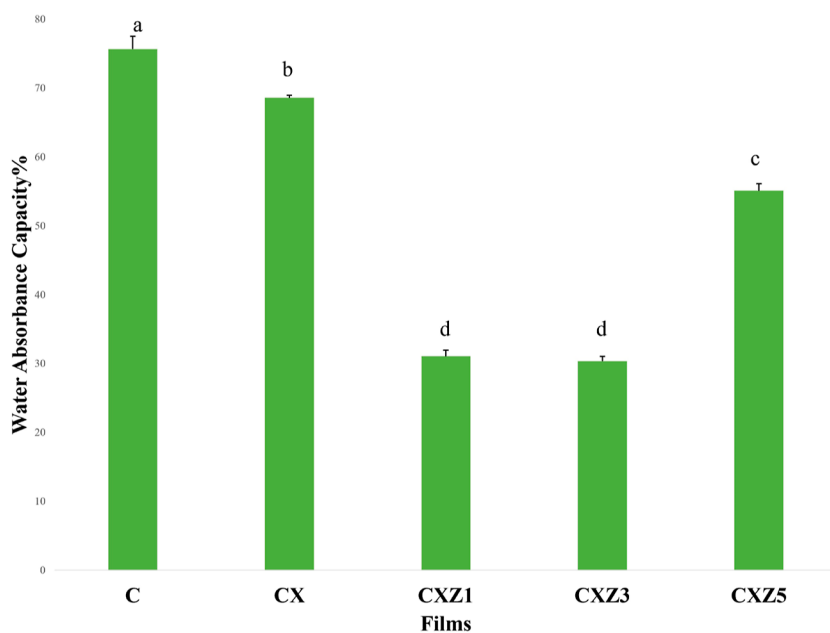


Figure 9. Water absorption capacity of all the films [means that do not share a letter are significantly different values at ($p \leq 0.05$) using the Tukey test (mean \pm SD, $n = 3$)] (C is the pure chitosan film, CX is the chitosan/xanthan gum blend film, CXZ1 is the chitosan/xanthan gum blend incorporated with 1 wt % ZnO nanoparticles, CXZ3 is the chitosan/xanthan gum blend incorporated with 3 wt % ZnO nanoparticles, and CXZ5 is the chitosan/xanthan gum blend incorporated with 5 wt % ZnO nanoparticles).

Water Vapor Transmission Rate. The rate of water vapor transmission of the film is one of the key elements that influence the shelf life of packaged food as the food item can readily decay owing to moisture absorption from the environment. Water resistance is important in determining film stability and the capacity to prevent the onset of microbiological deterioration of stored food. Hence, the packaging film should have a good moisture barrier. The WVTR for the manufactured films is tabulated in Table 2. As can be seen in Figure 8, due to its inherent hydrophilicity, the

pure chitosan film demonstrated the highest WVTR value of 560.934 ± 1.94 g/m²/day.^{38,57} The blend of chitosan and xanthan gum seems moderately hydrophilic, possessing about 11.88% less water vapor permeability compared to the pure chitosan film. This could be attributed to the interaction between the biopolymers and the formation of H bonds. Similar results were achieved by other scientists.^{22,24,25,56,58,59} FTIR spectroscopy results also suggest the same. The nanocomposite films, i.e., CXZ1, CXZ3, and CXZ5, showed decreases in the WVTR of 51.77, 54.95, and 47.17%,

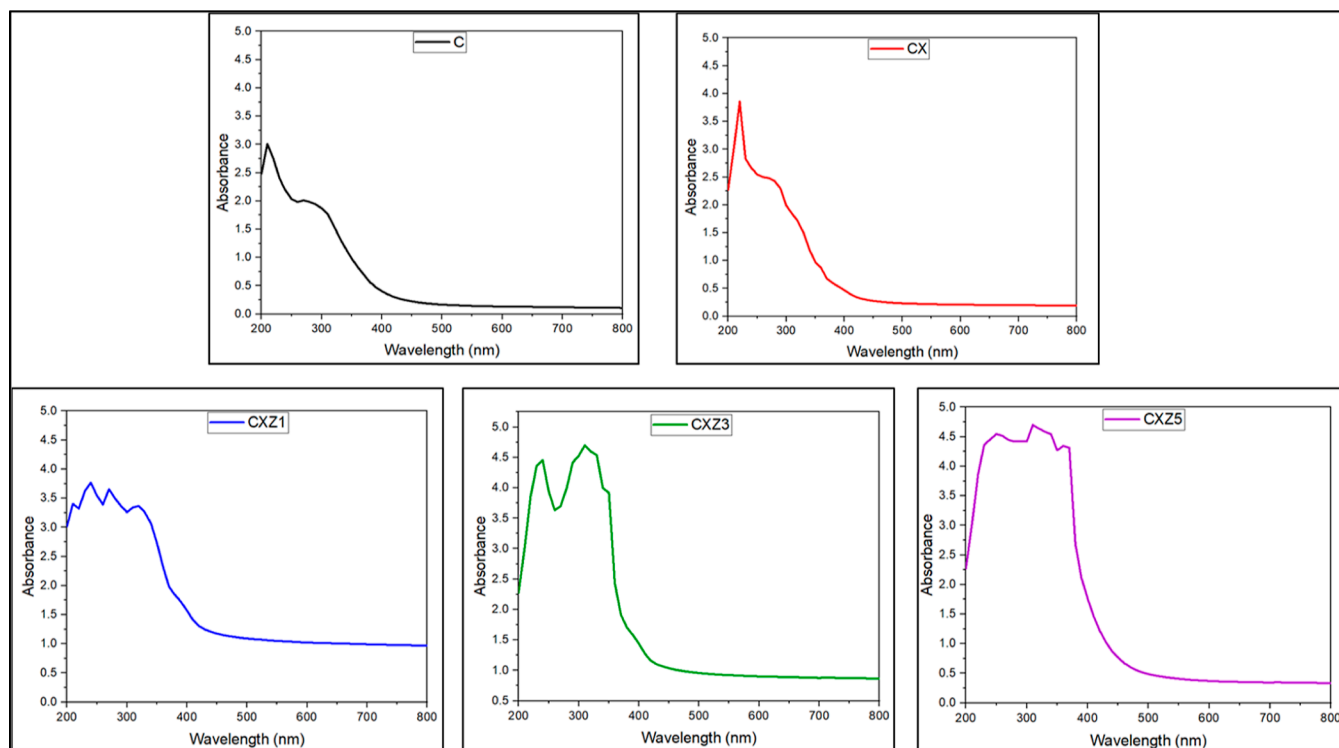


Figure 10. UV–visible spectra/UV barrier ability of the films (C is the pure chitosan film, CX is the chitosan/xanthan gum blend film, CXZ1 is the chitosan/xanthan gum blend incorporated with 1 wt % ZnO nanoparticles, CXZ3 is the chitosan/xanthan gum blend incorporated with 3 wt % ZnO nanoparticles, and CXZ5 is the chitosan/xanthan gum blend incorporated with 5 wt % ZnO nanoparticles).

respectively, compared to the pure biopolymer (chitosan) film. The addition of ZnO nanoparticles greatly decreased the WVTR of the nanocomposites, revealing that the nanoparticles had blocked the pores of the matrix, providing the polymeric films with improved levels of moisture and water resistance. Several other studies also have a similar claim that nanofiller reinforcement in the biopolymer or blends is responsible for the reduction of vapor diffusion, and it is mainly because of the nanofiller's less or impermeable nature that helps it gain better water barrier behavior.^{22,25,27,60,61}

Water Absorption Capacity. The Water absorption capacity test is a must for assessment so as to determine the water sensitivity of the film for its further practical uses. The collected findings are shown in Table 2 and Figure 9. The pure chitosan film had a higher water absorption capacity of $75.683 \pm 1.84\%$. Its water sensitivity was dramatically improved when xanthan gum was blended and ZnO nanoparticles were incorporated. Similar tendencies were also observed in the results presented by other researchers.²⁴ CXZ1 and CXZ3 films proved to have great water resistance with reduction in water absorption capacity of 58.94 and 59.88%, respectively, as compared to the control. The hydrophilic functional groups of chitosan (OH and NH₂) are the main reason behind its water absorption capacity.²⁴ However, the unavailability of these groups due to the interaction with the nanofillers resulted in decreased water absorption capacity in the nanocomposites. An earlier study on the cellulose nanocrystal/silver/alginate bionanocomposite by Yadav et al. also states that the lack of the presence of the –OH group of the biopolymer matrix due to H-bonding with nanofillers is responsible for decreased moisture absorption, as observed in two different composite films, i.e., the cellulose nanocrystal/Ag/alginate composite and cellulose nanocrystal-reinforced chitosan composite film.^{27,33}

On the other hand, Ni and co-workers suggested that ZnO nanoparticles have the ability to enhance hydrophobicity; their manufactured starch film supported this fact by decreasing the hydrophilicity of the film with the addition of 2 wt % ZnO nanoparticles.⁶²

Oxygen Transmission Rate and Permeability.

Although in the case of fresh fruits and vegetables that go through cellular respiration, complete prevention of gas permeability is not ideal,^{22,63} the presence of oxygen inside the packaging in a higher amount can shorten the shelf life of food because it can foster a favorable environment for microbial growth.⁶⁴ Oxygen transmission can result in oxidation (such as of lipid, vitamin, etc.), which damages sensory nutritional qualities in food and triggers several changes to food properties including taste, color, and other attributes. Acquiring nanocomposite packaging material with an adequate oxygen barrier aids in enhancing food quality and lengthening the shelf life. In general, the transmission of oxygen gas through the packaging film is dependent on its microstructure, void volume, structural arrangement of polymer chains, etc. Strong interactions and a well-organized hydrogen bonding network thereby can lower the OTR and OP values. The OTR and OP of the fabricated films are shown in Table 2. The OTR of the blended film (CX) compared to that of the pure chitosan film (C) decreased by 3.34% with the introduction of xanthan gum, which suggests an alteration in the interchain arrangement of the polymers owing to the interaction between both the biopolymers. Similar results were achieved by different researchers. Blending biopolymers is a popular strategy among scientists to improve their characteristics, including the gas barrier property.^{22,24} When compared to the C and CX films, the ZnO-reinforced nanocomposites showed a significant reduction in the OTR. This may have

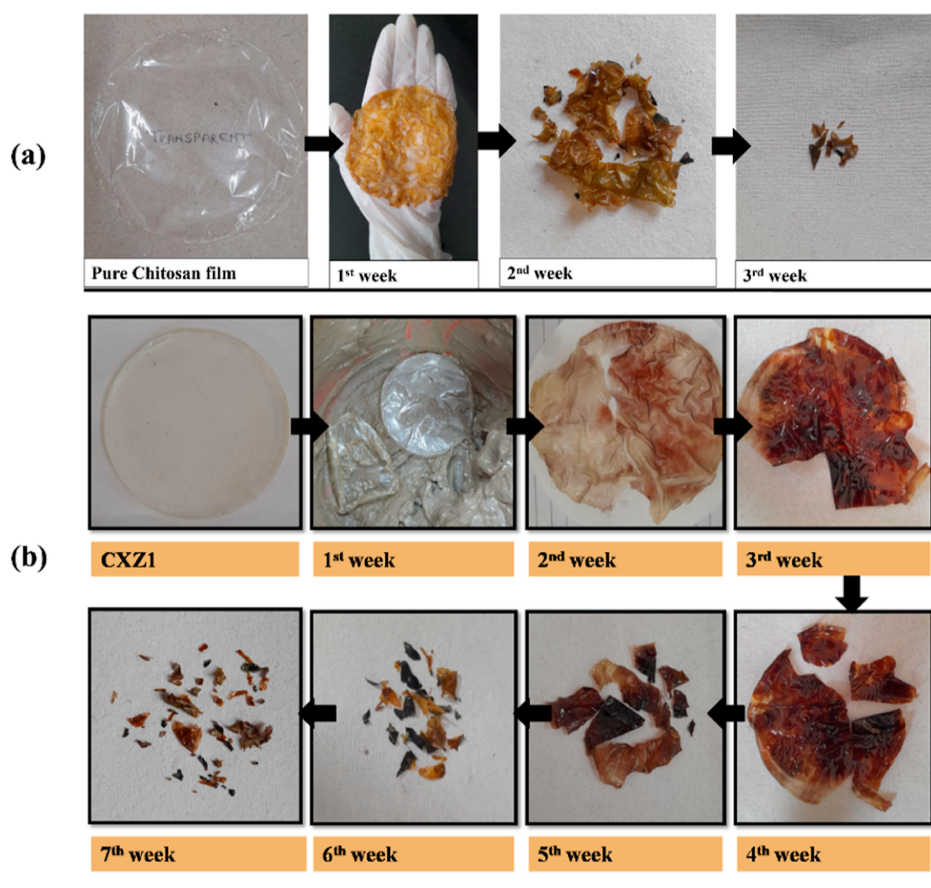


Figure 11. (a) Color changes and 89.53% weight loss of the pure chitosan film in the first 3 weeks. (b) Lowest degradation rate of the nanocomposite (CXZ1) film (chitosan/xanthan gum blend incorporated with 1 wt % ZnO nanoparticles) [all the pictures in this figure are original, taken and presented by the author Zeba Tabassum].

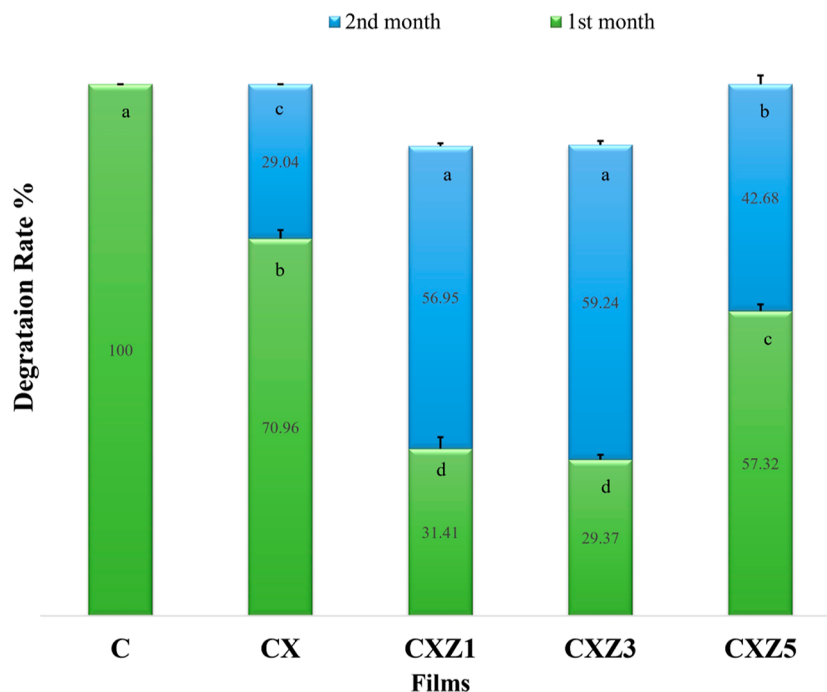


Figure 12. Degradation rate of all the films during the first 2 months [means that do not share a letter are significantly different values at ($p \leq 0.05$) using the Tukey test (mean \pm SD, $n = 3$)] (C is the pure chitosan film, CX is the chitosan/xanthan gum blend film, CXZ1 is the chitosan/xanthan gum blend incorporated with 1 wt % ZnO nanoparticles, CXZ3 is the chitosan/xanthan gum blend incorporated with 3 wt % ZnO nanoparticles, and CXZ5 is the chitosan/xanthan gum blend incorporated with 5 wt % ZnO nanoparticles).

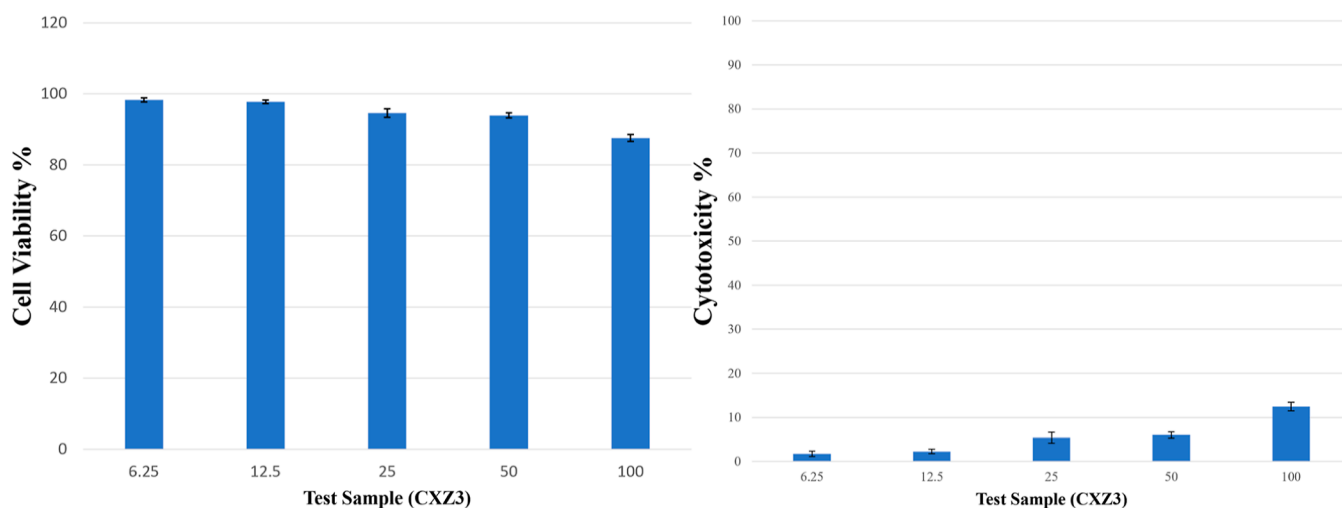


Figure 13. Cell viability and cytotoxicity % of film CXZ3 (chitosan/xanthan gum blend incorporated with 3 wt % ZnO nanoparticles).

happened as a result of increased molecular interaction leading to the creation of compact structures as well as the nanoparticles' ability to block pores.^{25,56} According to reports, the widely used commercial food packaging films made of low-density polyethylene and linear low-density polyethylene have limited oxygen barrier properties and a high oxygen penetration ($4000 \text{ cm}^3/\text{m}^2/\text{day}$). High OTR values often imply inadequate oxygen diffusion resistance through the packaging film, which will quickly cause microbial contamination of the packaged food. These findings suggested that the manufactured CXZ1 and CXZ3 films had a high potential for use as an effective packaging material to shield food from microorganisms.

OP of the film also depends on the surrounding environment, thickness of the film, etc. All the synthesized films (CX, CXZ1, CXZ3, and CXZ5) in this study showed a gradual increase in the OP value in contrast with that of the pure chitosan film with an increase in its thickness while considering 0.02308 atm at $25 \text{ }^\circ\text{C}$.

UV Barrier. Packaged foods can easily deteriorate, discolor, and undergo nutrient loss when exposed to UV and visible radiations. Therefore, the UV-screening capability of packaging is crucial in order to prevent such damages. The majority of synthetic polymeric food packaging films, such as low-density polyethylene and polypropylene, generally have poor UV light absorption.⁶⁵ The UV-visible absorption spectra of the fabricated films in the wavelength range of $200\text{--}800 \text{ nm}$ are shown in Figure 10. The pure chitosan film displayed the lowest absorption, whereas the fabricated nanocomposite film proved to have higher absorption, especially in the UV region, demonstrating that the film can serve as a strong UV barrier.²⁴ Addition of ZnO nanoparticles greatly influenced the UV-shielding property of the film. A similar claim was made by other researchers where they observed that ZnO-based nanocomposites have the potential to protect food from UV light.^{22,25}

Biodegradation. Biodegradable films do not contribute to pollution and thus do not become a threat to the environment. Polymeric materials undergo substantial alteration in the structure, morphology, and properties due to environmental elements including microbes, humidity, temperature, pH of the medium (soil), and other factors.¹¹ Fillers used in the film can also control the biodegradability and improve the durability of

the film due to either the formation of a compact structure and/or having an antimicrobial effect.⁶⁶ Soil burial biodegradability experiments show two-stage degradation, beginning with water diffusion into the film, which causes the films to swell and promotes the growth of microorganisms. The second step involves enzymatic and other secreted degradation, which results in weight loss and disruption of the film sample.²⁴ Changes in the weight and surface microstructure of the tested film aid in determining biodegradability. The bar graph in Figure 12 represents the weight loss of fabricated films subjected to microbial degradation, estimated in soil burial in laboratory conditions. All of the prepared films tested here for biodegradability have lost weight, had structural integrity changes, and went through bulk erosion type degradation.⁶⁷ In the first month, the pure chitosan (C) film entirely deteriorated (Figure 11a), whereas the CX film decayed by only around 70%. Hydrophilic polymeric films degrade faster and have a higher rate of weight loss in general. By readily invading, soil's moisture weakens the polymer network and makes the glycosidic connections vulnerable to hydrolysis. Indumathi and colleagues found their fabricated chitosan film to totally disintegrate within 1 month,²² whereas Hiremani et al. found the pure chitosan film to have a degradation rate of $78.34 \pm 2.00\%$ within the first 15 days.²⁴ Cassava flour-based bioplastic also displayed faster degradation because of its moisture uptake.⁶⁸ The ZnO bionanocomposite films synthesized in this study (CXZ1, CXZ3, and CXZ5) had 31.41, 29.37, and 57.32% weight loss in their soil burial biodegradation in the first month and 88.36, 88.61, and 100% at the end of the second month, respectively. This means the blending chitosan with xanthan gum and incorporating nanofillers enhanced the durability of the film to some extent due to their intermolecular interactions. The CXZ5 film has a faster degradation rate than the other two nanocomposites owing to the aggregation of nanoparticles, as evidenced by SEM analysis. Research suggests that nanofillers might also play a role in enhancing degradability in the case of their insufficient dispersion into the biopolymer matrix. After some weeks of soil burial of the bionanocomposite film, a dark spot started to appear in the film. A similar observation was stated by Krishnamurthy and Amrit Kumar for polylactic acid-based bioplastic.⁶⁹ However, then, gradually, the color of the whole film changed to dark brown, and a loss of transparency was

observed. The study reported by other researchers also supports this event.¹¹ The soil color likewise changed from brown to a form of blackish tone as time went on, and the film deteriorated. This supports the formation of humus and microbial degradation.⁷⁰ Kabir and co-workers also declared that microbial degradation alters the strength and color of polymeric material.⁶⁷

Cytotoxicity of the CXZ3 Film. CXZ3 seemed to be the best ratio film considering all the previous characterization results. According to the ISO 10993:5 standard procedure, the MTT assay was utilized to test the cytotoxicity of the CXZ3 film. Against L929 cells (mouse fibroblast cell lines), the sample's cytotoxicity was assessed. Figure 13 represents the film's cell viability and cytotoxicity against the L929 cell. The best nanocomposite film synthesized in this study (CXZ3) demonstrated outstanding cytocompatibility, with a cell survival of 87.56% and a cytotoxicity of 12.44% for the CXZ3 film. According to the GB/T 16886.5–2003 (ISO 10993-5:1999) analytical protocol, samples with a cell viability greater than 75% can be considered as noncytotoxic. So, it can be concluded that the chitosan/xanthan gum blend film reinforced with 3% ZnO nanoparticles proves itself as biocompatible.²⁵

CONCLUSIONS

In the current work, ZnO nanoparticle-incorporated chitosan/xanthan gum blended films were successfully fabricated by a simple and cost-effective solution casting technique. A number of instrumentation techniques were utilized to effectively characterize the films. FTIR spectroscopy analysis revealed that all inherent materials have interacted, leading to the generation of excellent miscibility. Xanthan gum blending with a chitosan matrix increases the tensile strength to certain limits. Further addition of ZnO nanoparticles imparts a positive impact, which enhances the film's mechanical property significantly both in terms of strength and flexibility. Barrier qualities, such as oxygen and moisture transmission rates, have decreased as compared to those of the pure chitosan film; additionally, the film also possesses a good UV shield. High degradability was observed and ensures that it is environmentally sustainable. The findings indicate that among all the prepared films, CXZ3 (chitosan/xanthan gum blend with 3% ZnO nanoparticles) was found to have the optimal formulation, demonstrating good physical and mechanical properties along with degradability under the natural condition. With all of the above-reported properties, it can be easily concluded that this film is a promising green biodegradable packaging material for food, making it a great substitute for the petroleum-based synthetic plastic packages.

AUTHOR INFORMATION

Corresponding Authors

Madhuri Girdhar – School of Bioengineering and Biosciences, Lovely Professional University, Phagwara 144401 Punjab, India; Email: madhuri.23745@lpu.co.in

Tabarak Malik – Department of Biomedical Sciences, Institute of Health, Jimma University, Jimma 0000, Ethiopia;

orcid.org/0000-0002-8332-7927;

Email: tabarak.malik@ju.edu.et

Anand Mohan – School of Bioengineering and Biosciences, Lovely Professional University, Phagwara 144401 Punjab, India; Email: anandmohan77@gmail.com

Authors

Zeba Tabassum – School of Bioengineering and Biosciences, Lovely Professional University, Phagwara 144401 Punjab, India

Anil Kumar – Gene Regulation Laboratory, National Institute of Immunology, New Delhi 110067, India

Complete contact information is available at:

<https://pubs.acs.org/10.1021/acsomega.3c03763>

Author Contributions

Zeba Tabassum: investigation; data curation; writing—original draft; and writing—review and editing. Madhuri Girdhar: project administration; supervision; and writing—review and editing. Anil Kumar: resources and writing—review and editing. Tabarak Malik: resources; supervision; and writing—review and editing. Anand Mohan: conceptualization; supervision; and writing—review and editing.

Notes

The authors declare no competing financial interest.

ACKNOWLEDGMENTS

We would like to thank the Central Instrumentation Facility, Lovely Professional University (CIF, LPU) for providing us the facility to perform FE-SEM and Stellixir Biotech Pvt. Ltd. for the MTT assay. We would like to extend our gratitude to IIT Delhi (CRF Sonipat campus) for providing the facility to utilize the universal testing machine (UTM).

REFERENCES

- (1) Akhter, M. S.; Khatun, H.; Hashem, M. A.; Rahman, M. M.; Khan, M. Effect of Storage Periods on the Quality and Shelf Life of Beef Liver at Refrigerated Temperature. *Meat Res.* **2022**, *2* (2), 1–5.
- (2) Zhang, M.; Biesold, G. M.; Choi, W.; Yu, J.; Deng, Y.; Silvestre, C.; Lin, Z. Recent Advances in Polymers and Polymer Composites for Food Packaging. *Mater. Today* **2022**, *53*, 134–161.
- (3) Tabassum, Z.; Mohan, A.; Mamidi, N.; Khosla, A.; Kumar, A.; Solanki, P. R.; Malik, T.; Girdhar, M. Recent Trends in Nanocomposite Packaging Films Utilising Waste Generated Biopolymers: Industrial Symbiosis and Its Implication in Sustainability. *IET Nanobiotechnol.* **2023**, *17*, 127–153.
- (4) Ncube, L. K.; Ude, A. U.; Ogunmuyiwa, E. N.; Zulkifli, R.; Beas, I. N. An Overview of Plastic Waste Generation and Management in Food Packaging Industries. *Recycling* **2021**, *6* (1), 12.
- (5) Tagrida, M.; Nilsuwan, K.; Gulzar, S.; Prodpran, T.; Benjakul, S. Fish Gelatin/Chitosan Blend Films Incorporated with Betel (Piper Betle L.) Leaf Ethanolic Extracts: Characteristics, Antioxidant and Antimicrobial Properties. *Food Hydrocolloids* **2023**, *137*, 108316.
- (6) Chinomso Iroegbu, A. O.; Ray, S. S. Lignin and Keratin-Based Materials in Transient Devices and Disposables: Recent Advances Toward Materials and Environmental Sustainability. *ACS Omega* **2022**, *7* (13), 10854–10863.
- (7) Majumder, R.; Das, A.; Mukherjee, A.; Kumar, S. Biopolymers: The Chemistry of Food and Packaging. *Biopolymer-Based Food Packaging: Innovations and Technology Applications*; Wiley, 2022; pp 29–65. DOI: [10.1002/9781119702313.ch2](https://doi.org/10.1002/9781119702313.ch2).
- (8) Mohan, A.; Girdhar, M.; Kumar, R.; Chaturvedi, H. S.; Vadhel, A.; Solanki, P. R.; Kumar, A.; Kumar, D.; Mamidi, N. Polyhydroxybutyrate-Based Nanocomposites for Bone Tissue Engineering. *Pharmaceuticals* **2021**, *14* (11), 1163.
- (9) Rodrigues, C.; de Mello, J. M. M.; Dalcanton, F.; Macuvelo, D. L. P.; Padoin, N.; Fiori, M. A.; Soares, C.; Riella, H. G. Mechanical, Thermal and Antimicrobial Properties of Chitosan-Based-Nanocomposite with Potential Applications for Food Packaging. *J. Polym. Environ.* **2020**, *28* (4), 1216–1236.

- (10) Cazón, P.; Velázquez, G.; Ramírez, J. A.; Vázquez, M. Polysaccharide-Based Films and Coatings for Food Packaging: A Review. *Food Hydrocolloids* **2017**, *68*, 136–148.
- (11) Vasile, C.; Pamfil, D.; Râpă, M.; Darie-Niță, R. N.; Mitelut, A. C.; Popa, E. E.; Popescu, P. A.; Draghici, M. C.; Popa, M. E. Study of the Soil Burial Degradation of Some PLA/CS Biocomposites. *Compos. B Eng.* **2018**, *142*, 251–262.
- (12) Priyadarshi, R.; Rhim, J.-W. Chitosan-Based Biodegradable Functional Films for Food Packaging Applications. *Innovat. Food Sci. Emerg. Technol.* **2020**, *62*, 102346.
- (13) Kumar, S.; Mukherjee, A.; Dutta, J. Chitosan Based Nanocomposite Films and Coatings: Emerging Antimicrobial Food Packaging Alternatives. *Trends Food Sci. Technol.* **2020**, *97*, 196–209.
- (14) Wang, H.; Qian, J.; Ding, F. Emerging Chitosan-Based Films for Food Packaging Applications. *J. Agric. Food Chem.* **2018**, *66* (2), 395–413.
- (15) Giannakas, A. E.; Leontiou, A. A. Montmorillonite Composite Materials and Food Packaging. *Composites Materials for Food Packaging*; Wiley, 2018; pp 1–71.
- (16) Girdhar, M.; Mohan, A.; Sharma, A. Blending Strategies of Natural Polymers: A Review Toxicity of Pesticides and Herbicides View Project Phytoremediation View Project. *Trends Biomater. Artif. Organs* **2016**, *30*, 61–76.
- (17) Souza, V.; Pires, J.; Vieira, É.; Coelho, I.; Duarte, M.; Fernando, A. Shelf Life Assessment of Fresh Poultry Meat Packaged in Novel Bionanocomposite of Chitosan/Montmorillonite Incorporated with Ginger Essential Oil. *Coatings* **2018**, *8* (5), 177.
- (18) Bhat, I. M.; Wani, S. M.; Mir, S. A.; Masoodi, F. A. Advances in Xanthan Gum Production, Modifications and Its Applications. *Biocatal. Agric. Biotechnol.* **2022**, *42*, 102328.
- (19) de Moraes Lima, M.; Bianchini, D.; Guerra Dias, A.; da Rosa Zavareze, E.; Prentice, C.; da Silveira Moreira, A. Biodegradable Films Based on Chitosan, Xanthan Gum, and Fish Protein Hydrolysate. *J. Appl. Polym. Sci.* **2017**, *134* (23), 44899 DOI: 10.1002/app.44899.
- (20) Chen, J.; Zheng, M.; Tan, K. B.; Lin, J.; Chen, M.; Zhu, Y. Development of Xanthan Gum/Hydroxypropyl Methyl Cellulose Composite Films Incorporating Tea Polyphenol and Its Application on Fresh-Cut Green Bell Peppers Preservation. *Int. J. Biol. Macromol.* **2022**, *211*, 198–206.
- (21) Ummartyotin, S.; Pechyen, C. Physico-Chemical Properties of ZnO and Chitosan Composite for Packaging Material. *J. Biobased Mater. Bioenergy* **2017**, *11* (3), 183–192.
- (22) Indumathi, M. P.; Saral Sarojini, K.; Rajarajeswari, G. R. Antimicrobial and Biodegradable Chitosan/Cellulose Acetate Phthalate/ZnO Nano Composite Films with Optimal Oxygen Permeability and Hydrophobicity for Extending the Shelf Life of Black Grape Fruits. *Int. J. Biol. Macromol.* **2019**, *132*, 1112–1120.
- (23) Patil, P. P.; Meshram, J. V.; Bohara, R. A.; Nanaware, S. G.; Pawar, S. H. ZnO Nanoparticle-Embedded Silk Fibroin-Polyvinyl Alcohol Composite Film: A Potential Dressing Material for Infected Wounds. *New J. Chem.* **2018**, *42* (17), 14620–14629.
- (24) Hiremani, V. D.; Gasti, T.; Masti, S. P.; Malabadi, R. B.; Chougale, R. B. Polysaccharide-Based Blend Films as a Promising Material for Food Packaging Applications: Physicochemical Properties. *Iran. Polym. J.* **2022**, *31* (4), 503–518.
- (25) Saral, S. K.; Indumathi, M. P.; Rajarajeswari, G. R. Mahua Oil-Based Polyurethane/Chitosan/Nano ZnO Composite Films for Biodegradable Food Packaging Applications. *Int. J. Biol. Macromol.* **2019**, *124*, 163–174.
- (26) Yadav, M.; Behera, K.; Chang, Y. H.; Chiu, F. C. Cellulose Nanocrystal Reinforced Chitosan Based UV Barrier Composite Films for Sustainable Packaging. *Polymers* **2020**, *12* (1), 202.
- (27) Yadav, M.; Liu, Y.-K.; Chiu, F.-C. Fabrication of Cellulose Nanocrystal/Silver/Alginate Bionanocomposite Films with Enhanced Mechanical and Barrier Properties for Food Packaging Application. *Nanomaterials* **2019**, *9* (11), 1523.
- (28) Homez-Jara, A.; Daza, L. D.; Aguirre, D. M.; Muñoz, J. A.; Solanilla, J. F.; Váquiro, H. A. Characterization of Chitosan Edible Films Obtained with Various Polymer Concentrations and Drying Temperatures. *Int. J. Biol. Macromol.* **2018**, *113*, 1233–1240.
- (29) Cazón, P.; Vázquez, M. Applications of Chitosan as Food Packaging Materials. *Sustainable Agriculture Reviews*; Springer, 2019; pp 81–123.
- (30) Xu, Y. X.; Kim, K. M.; Hanna, M. A.; Nag, D. Chitosan-Starch Composite Film: Preparation and Characterization. *Ind. Crops Prod.* **2005**, *21* (2), 185–192.
- (31) Souza, V. G. L.; Rodrigues, C.; Valente, S.; Pimenta, C.; Pires, J. R. A.; Alves, M. M.; Santos, C. F.; Coelho, I. M.; Fernando, A. L. Eco-Friendly ZnO/Chitosan Bionanocomposites Films for Packaging of Fresh Poultry Meat. *Coatings* **2020**, *10* (2), 110.
- (32) Saral, S. K.; Indumathi, M. P.; Rajarajeswari, G. R. Mahua Oil-Based Polyurethane/Chitosan/Nano ZnO Composite Films for Biodegradable Food Packaging Applications. *Int. J. Biol. Macromol.* **2019**, *124*, 163–174.
- (33) Yadav, M.; Behera, K.; Chang, Y.-H.; Chiu, F.-C. Cellulose Nanocrystal Reinforced Chitosan Based UV Barrier Composite Films for Sustainable Packaging. *Polymers* **2020**, *12* (1), 202.
- (34) Zhou, X.; Liu, X.; Liao, W.; Wang, Q.; Xia, W. Chitosan/Bacterial Cellulose Films Incorporated with Tea Polyphenol Nanoliposomes for Silver Carp Preservation. *Carbohydr. Polym.* **2022**, *297*, 120048.
- (35) Yadav, S.; Mehrotra, G. K.; Dutta, P. K. Chitosan Based ZnO Nanoparticles Loaded Gallic-Acid Films for Active Food Packaging. *Food Chem.* **2021**, *334*, 127605.
- (36) Siripatrawan, U.; Harte, B. R. Physical Properties and Antioxidant Activity of an Active Film from Chitosan Incorporated with Green Tea Extract. *Food Hydrocolloids* **2010**, *24* (8), 770–775.
- (37) Brugnerotto, J.; Lizardi, J.; Goycoolea, F. M.; Argüelles-Monal, W.; Desbrières, J.; Rinaudo, M. An Infrared Investigation in Relation with Chitin and Chitosan Characterization. *Polymers* **2001**, *42* (8), 3569–3580.
- (38) Sanuja, S.; Agalya, A.; Umamathy, M. J. Synthesis and Characterization of Zinc Oxide-Neem Oil-Chitosan Bionanocomposite for Food Packaging Application. *Int. J. Biol. Macromol.* **2015**, *74*, 76–84.
- (39) Roy, J. C.; Giraud, S.; Ferri, A.; Mossotti, R.; Guan, J.; Salaün, F. Influence of Process Parameters on Microcapsule Formation from Chitosan—Type B Gelatin Complex Coacervates. *Carbohydr. Polym.* **2018**, *198*, 281–293.
- (40) Li, L.-H.; Deng, J.-C.; Deng, H.-R.; Liu, Z.-L.; Xin, L. Synthesis and Characterization of Chitosan/ZnO Nanoparticle Composite Membranes. *Carbohydr. Res.* **2010**, *345* (8), 994–998.
- (41) Lee, S. W.; Said, N. S.; Sarbon, N. M. The Effects of Zinc Oxide Nanoparticles on the Physical, Mechanical and Antimicrobial Properties of Chicken Skin Gelatin/Tapioca Starch Composite Films in Food Packaging. *J. Food Sci. Technol.* **2021**, *58* (11), 4294–4302.
- (42) Nirmala, R.; Kim, H. Y.; Kalpana, D.; Navamathavan, R.; Lee, Y. S. Multipurpose Polyurethane Antimicrobial Metal Composite Films via Wet Cast Technology. *Macromol. Res.* **2013**, *21* (8), 843–851.
- (43) Butnaru, E.; Stoleru, E.; Brebu, M.; Darie-Nita, R.; Bargan, A.; Vasile, C. Chitosan-Based Bionanocomposite Films Prepared by Emulsion Technique for Food Preservation. *Materials* **2019**, *12* (3), 373.
- (44) Amini, E.; Valls, C.; Roncero, M. B. Promising Nanocomposites for Food Packaging Based on Cellulose - PCL Films Reinforced by Using ZnO Nanoparticles in an Ionic Liquid. *Ind. Crops Prod.* **2023**, *193*, 116246.
- (45) Hoque, M.; Sarkar, P.; Ahmed, J. Preparation and Characterization of Tamarind Kernel Powder/ZnO Nanoparticle-Based Food Packaging Films. *Ind. Crops Prod.* **2022**, *178*, 114670.
- (46) Suyatma, N. E.; Gunawan, S.; Putri, R. Y.; Tara, A.; Abbès, F.; Hastati, D. Y.; Abbès, B. Active Biohybrid Nanocomposite Films Made from Chitosan, ZnO Nanoparticles, and Stearic Acid: Optimization Study to Develop Antibacterial Films for Food Packaging Application. *Materials* **2023**, *16* (3), 926.

- (47) Dharini, V.; Periyar Selvam, S.; Jayaramudu, J.; Sadiku Emmanuel, R. Functional Properties of Clay Nanofillers Used in the Biopolymer-Based Composite Films for Active Food Packaging Applications - Review. *Appl. Clay Sci.* **2022**, *226*, 106555.
- (48) Wu, W.; Wu, Y.; Lin, Y.; Shao, P. Facile Fabrication of Multifunctional Citrus Pectin Aerogel Fortified with Cellulose Nanofiber as Controlled Packaging of Edible Fungi. *Food Chem.* **2022**, *374*, 131763.
- (49) de Oliveira, M. L. C.; Mirmehdi, S.; Scatolino, M. V.; Júnior, M. G.; Sanadi, A. R.; Damasio, R. A. P.; Tonoli, G. H. D. Effect of Overlapping Cellulose Nanofibrils and Nanoclay Layers on Mechanical and Barrier Properties of Spray-Coated Papers. *Cellulose* **2022**, *29* (2), 1097–1113.
- (50) Bumbudsanpharoke, N.; Ko, S. Nanoclays in Food and Beverage Packaging. *J. Nanomater.* **2019**, *2019*, 1–13.
- (51) Yadav, M.; Liu, Y. K.; Chiu, F. C. Fabrication of Cellulose Nanocrystal/Silver/Alginate Bionanocomposite Films with Enhanced Mechanical and Barrier Properties for Food Packaging Application. *Nanomaterials* **2019**, *9* (11), 1523.
- (52) Lomate, G. B.; Dandi, B.; Mishra, S. Development of Antimicrobial LDPE/Cu Nanocomposite Food Packaging Film for Extended Shelf Life of Peda. *Food Packag. Shelf Life* **2018**, *16*, 211–219.
- (53) Dehghani, S.; Peighambaroust, S. H.; Peighambaroust, S. J.; Hosseini, S. V.; Regenstein, J. M. Improved Mechanical and Antibacterial Properties of Active LDPE Films Prepared with Combination of Ag, ZnO and CuO Nanoparticles. *Food Packag. Shelf Life* **2019**, *22*, 100391.
- (54) Biswas, A.; Ahmed, T.; Rana, M. R.; Hoque, M. M.; Ahmed, M. F.; Sharma, M.; Sridhar, K.; Ara, R.; Stephen Inbaraj, B. Fabrication and Characterization of ZnO Nanoparticles-Based Biocomposite Films Prepared Using Carboxymethyl Cellulose, Taro Mucilage, and Black Cumin Seed Oil for Evaluation of Antioxidant and Antimicrobial Activities. *Agronomy* **2023**, *13* (1), 147.
- (55) Silvano, J. d. R.; Santa, R. A. A. B.; Martins, M. A. P. M.; Riella, H. G.; Soares, C.; Fiori, M. A. Nanocomposite of Erucamide-Clay Applied for the Control of Friction Coefficient in Surfaces of LLDPE. *Polym. Test.* **2018**, *67*, 1–6.
- (56) Soni, B.; Hassan, E. B.; Schilling, M. W.; Mahmoud, B. Transparent Bionanocomposite Films Based on Chitosan and TEMPO-Oxidized Cellulose Nanofibers with Enhanced Mechanical and Barrier Properties. *Carbohydr. Polym.* **2016**, *151*, 779–789.
- (57) Indumathi, M. P.; Saral Sarojini, K.; Rajarajeswari, G. R. Antimicrobial and Biodegradable Chitosan/Cellulose Acetate Phthalate/ZnO Nano Composite Films with Optimal Oxygen Permeability and Hydrophobicity for Extending the Shelf Life of Black Grape Fruits. *Int. J. Biol. Macromol.* **2019**, *132*, 1112–1120.
- (58) Uthaya Kumar, U. S.; Abdulmadjid, S. N.; Olaiya, N. G.; Amirul, A. A.; Rizal, S.; Rahman, A. A.; Alfatah, T.; Mistar, E. M.; Abdul Khalil, H. P. S. Extracted Compounds from Neem Leaves as Antimicrobial Agent on the Physico-Chemical Properties of Seaweed-Based Biopolymer Films. *Polymers* **2020**, *12* (5), 1119.
- (59) Zhang, W.; Sani, M. A.; Zhang, Z.; McClements, D. J.; Jafari, S. M. High Performance Biopolymeric Packaging Films Containing Zinc Oxide Nanoparticles for Fresh Food Preservation: A Review. *Int. J. Biol. Macromol.* **2023**, *230*, 123188.
- (60) Noshirvani, N.; Ghanbarzadeh, B.; Rezaei Mokarram, R.; Hashemi, M. Novel Active Packaging Based on Carboxymethyl Cellulose-Chitosan-ZnO NPs Nanocomposite for Increasing the Shelf Life of Bread. *Food Packag. Shelf Life* **2017**, *11*, 106–114.
- (61) Mujeeb Rahman, P.; Abdul Mujeeb, V. M.; Muraleedharan, K.; Thomas, S. K. Chitosan/Nano ZnO Composite Films: Enhanced Mechanical, Antimicrobial and Dielectric Properties. *Arab. J. Chem.* **2018**, *11* (1), 120–127.
- (62) Ni, S.; Zhang, H.; Godwin, P. M.; Dai, H.; Xiao, H. ZnO Nanoparticles Enhanced Hydrophobicity for Starch Film and Paper. *Mater. Lett.* **2018**, *230*, 207–210.
- (63) Robertson, G. L. *Food Packaging*; CRC Press, 2005.
- (64) Ariyaratna, I. R.; Rajakaruna, R. M. P. I.; Karunaratne, D. N. The Rise of Inorganic Nanomaterial Implementation in Food Applications. *Food Control* **2017**, *77*, 251–259.
- (65) Ramos, Ó. L.; Reinas, I.; Silva, S. L.; Fernandes, J. C.; Cerqueira, M. A.; Pereira, R. N.; Vicente, A. A.; Poças, M. F.; Pintado, M. E.; Malcata, F. X. Effect of Whey Protein Purity and Glycerol Content upon Physical Properties of Edible Films Manufactured Therefrom. *Food Hydrocolloids* **2013**, *30* (1), 110–122.
- (66) Neibolts, N.; Platnieks, O.; Gaidukovs, S.; Barkane, A.; Thakur, V. K.; Filipova, I.; Mihai, G.; Zelca, Z.; Yamaguchi, K.; Enachescu, M. Needle-Free Electrospinning of Nanofibrillated Cellulose and Graphene Nanoplatelets Based Sustainable Poly (Butylene Succinate) Nanofibers. *Mater. Today Chem.* **2020**, *17*, 100301.
- (67) Kabir, E.; Kaur, R.; Lee, J.; Kim, K.-H.; Kwon, E. E. Prospects of Biopolymer Technology as an Alternative Option for Non-Degradable Plastics and Sustainable Management of Plastic Wastes. *J. Clean. Prod.* **2020**, *258*, 120536.
- (68) Wahyuningtyas, N.; Suryanto, H. Analysis of Biodegradation of Bioplastics Made of Cassava Starch. *J. Mech. Eng. Sci. Technol.* **2017**, *1* (1), 24–31.
- (69) Krishnamurthy, A.; Amritkumar, P. Synthesis and Characterization of Eco-Friendly Bioplastic from Low-Cost Plant Resources. *SN Appl. Sci.* **2019**, *1* (11), 1432.
- (70) Rachmawati, N.; Triwibowo, R.; Widiyanto, R. Mechanical Properties and Biodegradability of Acid-Soluble Chitosan-Starch Based Film. *Bull. Mar. Fish. Postharvest Biotechnol.* **2015**, *10* (1), 1.